RED CELLS, IRON, AND ERYTHROPOIESIS

The common hereditary elliptocytosis-associated α-spectrin L260P mutation perturbs erythrocyte membranes by stabilizing spectrin in the closed dimer conformation

Sandra L. Harper,[1] Sira Sriswasdi,[1,2] Hsin-Yao Tang,[1] Massimiliano Gaetani,[3] Patrick G. Gallagher,[4] and David W. Speicher[1,2]

[1]The Center for Systems and Computational Biology and Molecular and Cellular Oncogenesis Program, The Wistar Institute, Philadelphia, PA; [2]Genomics and Computational Biology Graduate Group, University of Pennsylvania, Philadelphia, PA; [3]Ri.MED Foundation, Regenerative Medicine and Biomedical Technologies Unit at ISMETT, Palermo, Italy; and [4]Yale University School of Medicine, New Haven, CT

Key Points

- The common HE mutation αL260P reduces spectrin tetramer links between junctional complexes in red cell membranes by favoring closed dimers.
- Favoring closed spectrin dimer formation is a new mechanism of red cell membrane destabilization by hereditary anemia mutations.

Hereditary elliptocytosis (HE) and hereditary pyropoikilocytosis (HPP) are common disorders of erythrocyte shape primarily because of mutations in spectrin. The most common HE/HPP mutations are located distant from the critical αβ-spectrin tetramerization site, yet still interfere with formation of spectrin tetramers and destabilize the membrane by unknown mechanisms. To address this question, we studied the common HE-associated mutation, αL260P, in the context of a fully functional mini-spectrin. The mutation exhibited wild-type tetramer binding in univalent binding assays, but reduced binding affinity in bivalent-binding assays. Biophysical analyses demonstrated the mutation-containing domain was only modestly structurally destabilized and helical content was not significantly changed. Gel filtration analysis of the αL260P mini-spectrin indicated more compact structures for dimers and tetramers compared with wild-type. Chemical crosslinking showed structural changes in the mutant mini-spectrin dimer were primarily restricted to the vicinity of the αL260P mutation and indicated large conformational rearrangements of this region. These data indicate the mutation increased the stability of the closed dimer state, thereby reducing tetramer assembly and resulting in membrane destabilization. These results reveal a novel mechanism of erythrocyte membrane destabilization that could contribute to development of therapeutic interventions for mutations in membrane proteins containing spectrin-type domains associated with inherited disease. (*Blood*. 2013;122(17):3045-3053)

Introduction

The hereditary elliptocytosis (HE) syndromes are the most common disorders of erythrocyte shape. In parts of Africa, the incidence of HE approaches that of sickle cell disease, presumably because HE red cells confer some resistance to invasion by malaria parasites. Most cases of HE are due to missense mutations in the erythrocyte membrane skeleton protein spectrin.[1,2]

Spectrin is a critical component of the erythrocyte membrane skeleton, a network of proteins on the cytoplasmic face of the membrane that maintains the shape and elasticity of the red cell membrane.[3,4] In the erythrocyte, spectrin exists as an antiparallel αβ-heterodimer that self-associates in a head-to-head fashion to form tetramers and higher order oligomers.[5] Studies of spectrin mutations in HE and the related disorder hereditary pyropoikilocytosis (HPP)[6,7] have provided important insights into the structure and function of spectrin in the cell.[8] Furthermore, erythrocyte spectrin has served as the paradigm for our understanding of spectrin proteins in nonerythroid cells. We now know that spectrin mutations in other cell types play important roles in pathogenesis of several disease phenotypes, including a number of neurologic disorders.[9-11]

In the erythrocyte, α-spectrin is an ~280-kDa polypeptide comprising 20 homologous ~106 amino acid "spectrin-type homologous domains" often called "spectrin repeats," an N-terminal partial repeat, an SH3 domain, and a C-terminal EF hand domain. β-Spectrin is an ~246-kDa polypeptide comprising 16 complete repeat units, a partial repeat near the C terminus, an N-terminal actin binding domain, and a nonhomologous phosphorylated C-terminal domain (Figure 1A). Spectrin tetramers are anchored to the membrane through ankyrin[12-14] and an actin-based junctional complex. Crystal structures of up to 3 or 4 tandem spectrin type domains have been determined, and all of these domains are 3-helix bundles interconnected by short helical segments.[15-19]

Many HE and HPP mutations are in the tetramerization domain comprising the α0 and β17 partial domains, and these mutations

Submitted February 28, 2013; accepted August 15, 2013. Prepublished online as *Blood* First Edition paper, August 23, 2013; DOI 10.1182/blood-2013-02-487702.

S.L.H. and S.S. contributed equally to this study.

The online version of this article contains a data supplement.

There is an Inside *Blood* commentary on this article in this issue.

The publication costs of this article were defrayed in part by page charge payment. Therefore, and solely to indicate this fact, this article is hereby marked "advertisement" in accordance with 18 USC section 1734.

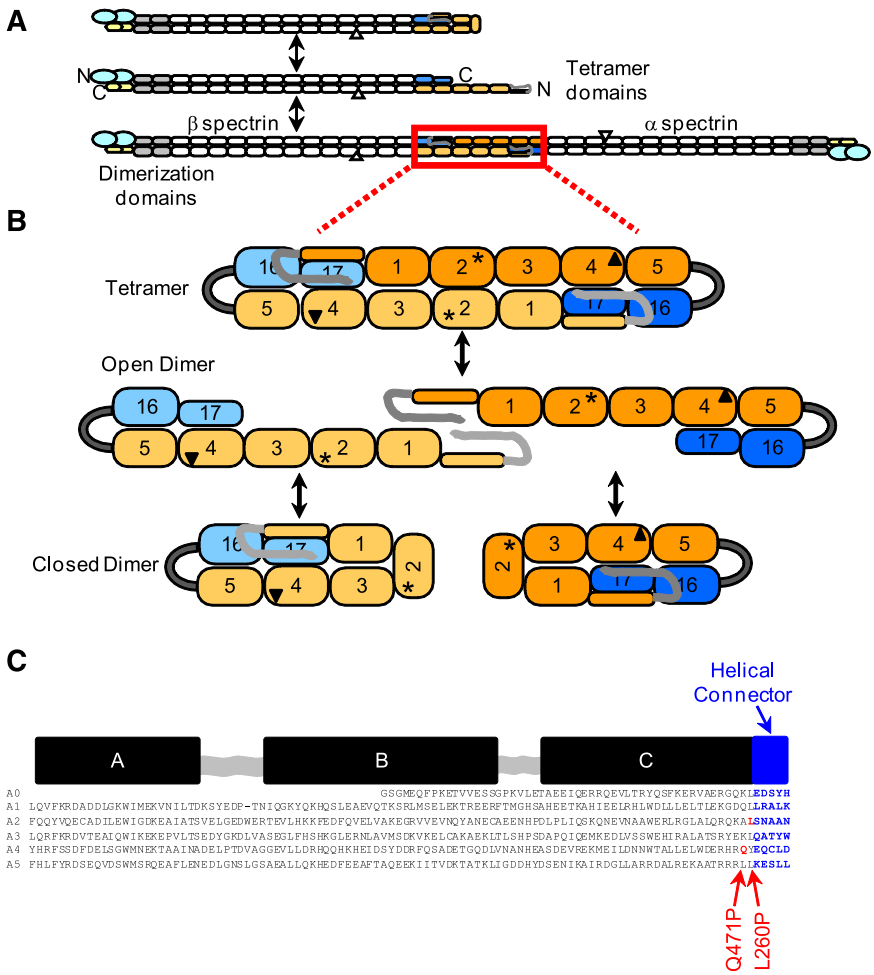

Figure 1. Schematic representation of erythrocyte spectrin equilibria and distal mutations. (A) Full-length red cell spectrin illustrating the closed dimer ↔ open dimer ↔ tetramer equilibria and component domains. The homologous ~106 residue spectrin type "repeat units" that comprise most of the spectrin molecule are represented by rounded rectangles. The gray rectangles are domains required to initiate antiparallel lateral heterodimer assembly.[50] The α-spectrin EF hands are represented by small yellow hexagons and the laterally associated actin binding domain at the N terminus of β-spectrin is represented by larger blue ovals. The SH3 domain (α10) inserted with the α9 domain is indicated by a small white triangle. The domains used in the construction of the recombinant mini-spectrin are highlighted in light blue and wheat and orange and blue. (B) Mini-spectrin in its tetramer form and the corresponding dissociation to open dimer and conversion to closed dimers. The α0-5 is connected to β16-17 using a short glycine linker (gray arc). The approximate locations of the L260P (asterisk) and Q471P (triangle) mutations are shown. (C) The relationship between the secondary structure of the 3-helix bundle motif and the α0-5 spectrin sequence. The black bars above the sequences indicate the locations of the A, B, and C helices of the 3-helix bundle that comprises each repeat, the gray-shaded squiggles indicate locations of loop regions, and the blue-shaded bar and sequence indicate the helical linker region that connects the end of the C helix to the beginning of the A helix in the next repeat. The locations of the L260P and Q471P mutations in the sequence are highlighted in red.

reduce or abolish tetramer formation either through destabilization of protein folding or disrupting protein-protein contacts in the contact interface.[20,21] However, in many cases, pathogenic mutations are located large distances (100 Å or more) from the tetramerization site and are thought to exert destabilizing effects on tetramer formation through poorly understood mechanisms. These include the 3 most common HE-associated α-spectrin mutations found worldwide: dupL154, L260P, and L207P.[22-24] Two of these common mutations insert helix-breaking proline residues into α-helical segments of spectrin repeats. Study of a rare distal mutation, αQ471P, located adjacent to the linker between the α4 and α5 repeats, revealed this mutation decoupled these 2 repeat domains, causing them to unfold near physiological temperature. This suggested that these domains would prematurely unfold under moderate tensile stress, resulting in destabilization of the actin crosslinks provided by the spectrin tetramers.[25]

In the current study, we analyzed the common HE αL260P mutation[26] located adjacent to the linker between the α2 and α3 repeats. Because this mutation was in an analogous structural position within spectrin repeats to the αQ471P mutation (Figure 1C), we hypothesized that a similar mechanism would contribute to destabilization of spectrin tetramers and red cell membranes. Surprisingly, initial results indicated a different mechanism was involved; therefore, a detailed evaluation of the αL260P mutation was pursued using a mini-spectrin construct capable of forming closed dimers, open dimers, and bivalent tetramers analogous to full-length spectrin (Figure 1B).[27] The L260P mutant protein showed reduced capacity to form tetramers in bivalent tetramerization assays, suggesting that perturbations in the closed dimer-open dimer equilibrium played an important role in tetramer assembly. Chemical crosslink analyses revealed mutant-specific crosslinks in the vicinity of the mutation, indicative of large conformational rearrangements that stabilized closed dimers. Shifting the equilibrium from tetramers to closed dimers would reduce the amount of tetramers on the membrane, a new mechanism of HE-associated red cell membrane destabilization, and one that differs markedly from the Q471P mutation.

Elucidation of these multiple mechanisms underlying the pathobiology of membrane dysfunction in HE and HPP provides essential knowledge required for potential development of future therapeutic interventions for these diseases.

Materials and methods

Expression and purification of recombinant mini-spectrin protein

The expression and purification of the wild-type (WT) construct used in this study have been described previously.[27] Site-directed mutagenesis was used to introduce the HE-associated mutation L260P into the mini-spectrin construct. The purification of the L260P mutant protein followed the same procedure as the WT protein. Expression and purification of the α0-5 and β16-17 constructs followed a similar purification scheme.

Biophysical measurements

Differential scanning calorimetry, circular dichroism, sedimentation equilibrium analysis, and isothermal titration calorimetry were performed as previously described.[21,27]

Analytical gel filtration

The WT and L260P dimers and tetramers were isolated and evaluated by gel filtration chromatography using 2 G4000SW$_{XL}$ BioAssist columns (Tosoh Corp.) connected in series and maintained at room temperature (20-23°C). After initial isolation of the tetramer or dimer, the sample was diluted to 0.05 mg/mL and then 100 pmol was reinjected immediately or incubated at 37°C and reinjected at 45-minute intervals.

Crosslinking reactions

Crosslinking reactions were performed using a freshly prepared solution of 1-ethyl-3-(3-dimethylaminopropyl)carbodiimide (EDC)/sulfo-*N*-hydroxysulfosuccininimide (sulfo-NHS). The WT and L260P dimers and tetramers were isolated by gel filtration in 10 mM phosphate and 130 mM sodium chloride; pH 7.3. Sample concentrations were adjusted to 0.2 mg/mL with the same buffer. Reactions containing 10 mM EDC/5 mM sulfo-NHS were incubated at 0°C. Reactions containing 2.5 mM EDC/1.25 mM sulfo-NHS were incubated at room temperature (20-23°C). Aliquots of each sample were removed at 30, 60, and 120 minutes and quenched by addition of 20 mM dithiothreitol (final concentration) followed by incubation at the same temperature for 15 minutes. After quenching, samples were buffer exchanged and concentrated using Amicon Ultra Ultracel-50K filter units (Millipore Corp.) before sodium dodecyl sulfate–polyacrylamide gel electrophoresis (SDS-PAGE).

SDS-PAGE and trypsin digestion

For each crosslinked sample (oligomer state, temperature, and time point), multiple lanes loaded with 6 μg/lane were separated on 3% to 8% Tris-Acetate mini-gels (Life Technologies) in Tris acetate running buffer and stained with colloidal Coomassie Blue. Bands corresponding to control, crosslinked dimer, or crosslinked tetramer were excised, alkylated, and digested with trypsin.

LC-MS/MS

Liquid chromatography tandem mass spectrometry (LC-MS/MS) analysis was performed on an LTQ-Orbitrap XL mass spectrometer (Thermo Scientific) coupled with a Nano-ACQUITY UPLC system (Waters) as previously described,[28] with minor modifications. Briefly, charge-state screening was enabled to reject +1 and +2 ions. Lists of expected mass to charge ratio and retention time ranges for candidate crosslinks identified in the discovery run were subsequently used in targeted LC-MS/MS analyses to identify additional crosslinks. Monoisotopic precursor selection was disabled, precursor mass tolerance was set at 20 ppm, and MS/MS threshold was set at 10 000 ion counts for low-resolution MS/MS and 50 000 ion counts for high-resolution scans. Resolution was set to 15 000 for both full scans and MS/MS scans. Isolation width was increased from 2.5 to 4 mass to charge ratio for high-resolution scans to compensate for space-charging.

Identification of crosslinked peptides

Label-free comparisons of the discovery LC-MS/MS data were performed on the Rosetta Elucidator system to identify peptide signals that were enriched in the crosslink samples as previously described.[28,29] Precursor signals that were at least 10-fold enriched in 1 of the crosslink samples (relative to control) were retained as crosslink candidates. Using a mass tolerance of 5 ppm, the mass list of these candidates was compared with mass lists of theoretical crosslinks generated via in silico trypsin digestion and crosslinking of the pertinent mini-spectrin sequence. Custom software was used to evaluate the correlation between low-resolution MS/MS spectra and theoretical crosslinked peptide amino acid sequences, to create target lists for high-resolution MS/MS data acquisition, and to perform a final analysis on the resulting spectra (Sriswasdi S, Harper SL, Tang HY, and Speicher DW, manuscript in preparation). Automatically generated, graphically annotated spectra, along with correlation quality scores, were used to identify crosslinked peptides and pinpoint specific crosslinked sites.

Table 1. Tetramer binding using univalent and divalent recombinant proteins

Recombinant	Univalent K_d (ITC)*		Divalent K_d (SE)†	
	23°C	30°C	23°C	30°C
WT	0.5 μM	1.8 μM	0.1 μM	1 μM
L260P	0.4 μM	0.8 μM	1.2 μM	5 μM
Q471P	0.4 μM	0.7 μM	0.2 μM	1 μM

ITC, isothermal titration calorimetry; SE, sedimentation equilibrium.

*ITC was used to measure the univalent binding of WT, L260P, or Q471P α0-5 titrated into β16-17.

†SE was used to measure the divalent dimer-tetramer equilibrium of WT, L260P, and Q471P mini-spectrins.

Modeling large structural rearrangement in L260P tetramer

Homology modeling was performed using MODELER, as previously described.[30-34] The portion of a WT mini-spectrin tetramer model encompassing 3 long-range L260P-specific crosslinks, α2-3-4/β17α0-1-2, was used as the starting structure. Distances between crosslinked Cα residues in this region were constrained by imposing upper bounds for physical distances at 11.0 Å with a standard deviation of 0.1 Å. In each scenario, 100 models were generated and the structure with the lowest pairwise root-mean-square deviation was chosen.

Results

Characterization of the HE-related L260P mutant

The effects of the αL260P mutation on tetramer formation were initially evaluated using α0-5 and β16-17 recombinant polypeptides in an isothermal titration calorimetry binding assay at 23°C and 30°C. Isothermal titration calorimetry characterizes properties of biomolecule interactions in solution, particularly the binding affinity. We used this technique to measure the capacity of WT and mutant recombinant fragments to form univalent associations at the tetramerization site. Interestingly, this mutant exhibited binding affinities that were similar to the corresponding WT peptides (Table 1). Similarly, the Q471P mutant exhibited normal tetramer binding affinity.[25] In contrast, prior analyses of HE and HPP mutations located within the α0 and β17 tetramerization binding site showed reduced tetramer binding for most mutations when a similar univalent tetramer binding assay was used.[21] The normal binding affinity for these distal mutants in univalent tetramer-binding assays suggested the need for more complex recombinant constructs capable of undergoing the entire set of interactions encountered in full-length spectrin. A previous study demonstrated that a WT mini-spectrin recombinant protein comprising α0-5 linked to β16-17 recapitulated tetramer binding and structural properties.[27] Specifically, this mini-spectrin showed identical tetramer binding affinity at 30°C to that of full-length spectrin purified from fresh human erythrocytes, which had a dissociation constant (K_d) of approximately 1 μM.[35,36] These similarities indicated the mini-spectrin was a suitable template for studying distal mutations in a more physiological context than provided by univalent head-to-head tetramer binding assays.

The relationships of full-length spectrin and the WT mini-spectrin construct as well as the respective closed dimer ↔ open dimer ↔ tetramer equilibria are shown in Figure 1. The locations of the L260P (asterisk) and the Q471P (triangle) mutations are shown on the

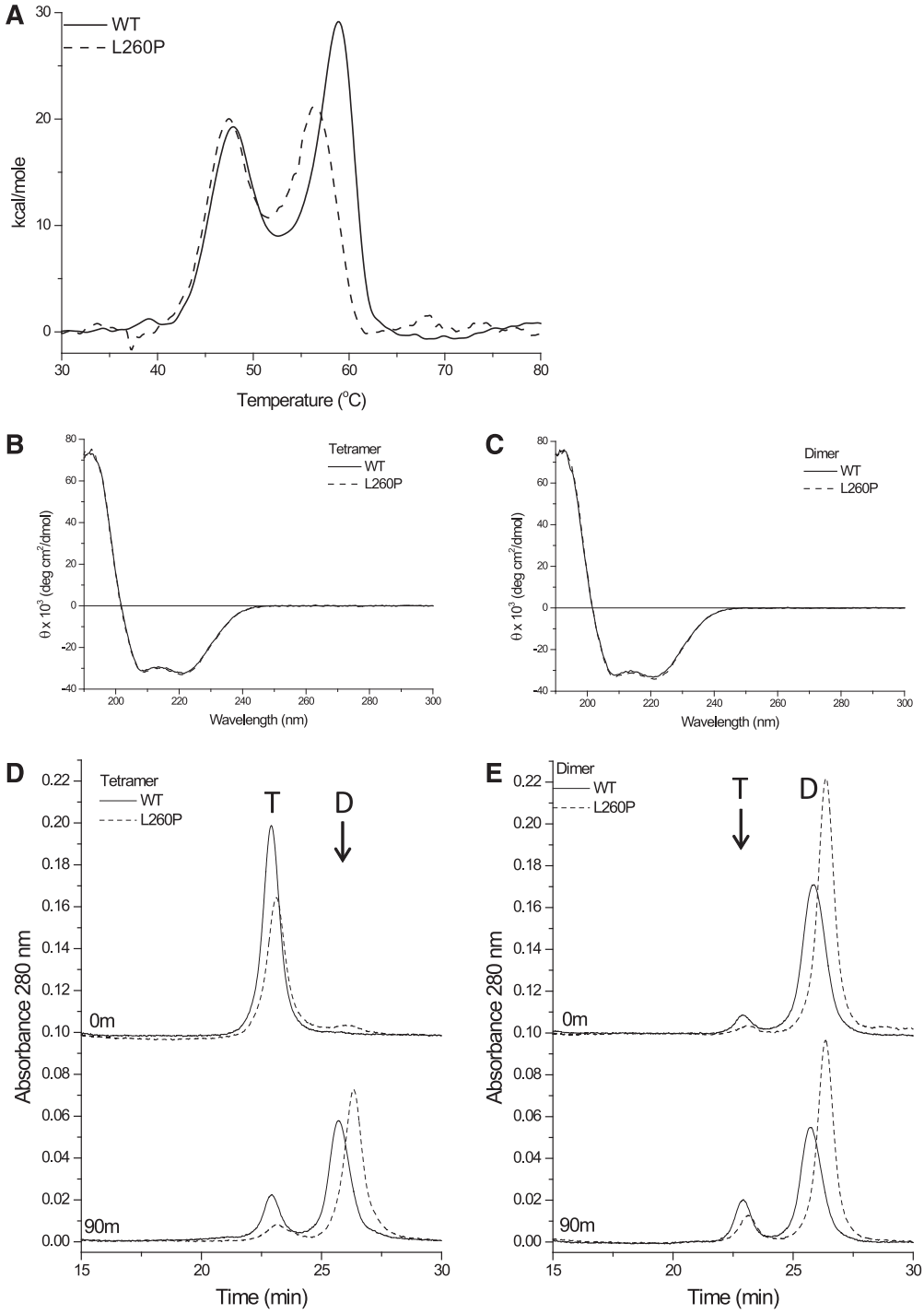

Figure 2. Structural properties of WT and L260P mini-spectrins. (A) Representative differential scanning calorimetry (DSC) scans of WT and L260P tetramers. DSC analysis was performed in 10 mM sodium phosphate, 130 mM NaCl, and 1 mM Tris(2-carboxyethyl)-phosphine hydrochloride (TCEP) pH 7.4 using a scan rate of 30°C/h over the temperature range of 20-90°C at a protein concentration of 0.5 mg/mL. (B) Representative circular dichroism (CD) results from WT and L260P tetramer. CD analysis was performed in 10 mM sodium phosphate, 130 mM sodium fluoride, and 0.1 mM TCEP pH 7.4 using a protein concentration of 0.16 mg/mL. (C) CD analysis of WT and L260P dimers at 0.18 mg/mL. (D) A total of 100 pmol mini-spectrin tetramer injected immediately after isolation at 4°C in 10 mM sodium phosphate, 130 mM sodium chloride, 0.1 mM EDTA, 0.15 mM phenylmethylsulfonyl fluoride, 1 mM TCEP pH 7.0 (upper panel), and after 90 minutes' incubation at 37°C (lower panel). (E) A total of 100 pmol mini-spectrin dimers injected immediately after isolation at 4°C (upper panel) and after 90 minutes' incubation at 37°C (lower panel).

mini-spectrin schematic. Both mutations are located at the end of the C-helix immediately adjacent to the interdomain linker region (Figure 1C). Because each spectrin type repeat (rounded rectangles) is approximately 50 Å in length, the L260P and Q471P mutations are at least 100 Å and 200 Å, respectively, from the tetramer binding site on the same polypeptide chain.

Using the mini-spectrin template, the L260P and Q471P mutants were compared with the WT protein using sedimentation equilibrium, which is another technique used to measure binding affinities of biomolecules. Sedimentation equilibrium is more appropriate than isothermal titration calorimetry when the interacting species are very large and of similar size, as is the case here, where 2 identical dimers

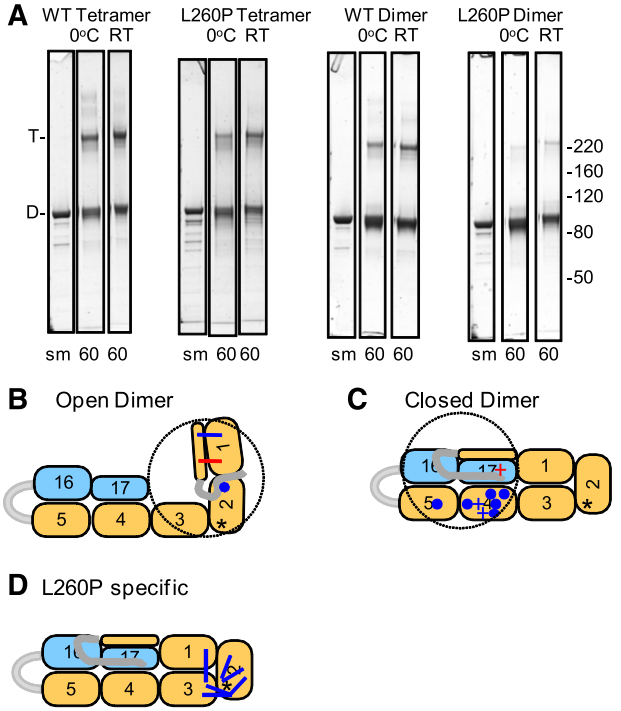

Figure 3. Chemical crosslinking of mini-spectrin tetramers and dimers. (A) SDS-PAGE gel showing the mini-spectrin samples before and after crosslinking with EDC/NHS. The 60-minute time point is shown for each condition (complete time courses are shown in supplemental Figure 3). (B-D) Asterisk indicates the location of the L260P mutation, the dotted circle represents a distance of 50 Å from the N terminus end of the α0 helix that defines the maximum extension of the 20 residues in the disordered "tail" preceding the α0 helix; blue lines indicate approximate locations of crosslinks observed at 0°C and room temperature (RT); blue dots indicate sites to which the α-N terminus was observed to be crosslinked at 0°C and RT. The red lines represent crosslinks only observed at RT. (B) Crosslinks indicative of an open dimer conformation. (C) Crosslinks indicative of a closed dimer conformation. Circles are common to WT and L260P and + are specific to L260P. The red + is only observed at RT. (D) Crosslinks specific to the L260P dimer.

form a tetramer. This technique was used to measure the bivalent binding affinity of the WT and mutant mini-spectrins. The apparent K_d of 1 μM for the WT dimer-tetramer association was confirmed and an apparent K_d of 5 μM at 30°C was obtained for the L260P mutant, indicating a fivefold weaker binding affinity. In contrast, the Q471P mutant continued to exhibit binding affinity equivalent to the WT protein in this divalent assay. Experiments performed at 23°C showed a similar trend of weaker binding affinity for L260P compared with the WT or Q471P mini-spectrins, although for each construct the binding affinity was stronger at the lower temperature (Table 1; supplemental Figure 1), consistent with the known temperature effects on tetramer formation of full-length spectrin.[37] This weaker binding affinity of the L260P mini-spectrin is consistent with prior analyses of full-length spectrin isolated from L260P erythrocytes, which showed normal amounts of total spectrin, but a relative decrease in the tetramer to dimer ratio.[38]

Thermal stability and secondary structural characteristics of the WT and L260P proteins were determined using differential scanning calorimetry (DSC) and circular dichroism. DSC measures temperature-induced unfolding of protein domains and is therefore an indicator of protein stability because more stable structures unfold at higher temperatures. Representative DSC scans are shown in Figure 2A. Scans of the WT protein showed 2 peaks, 1 with a melting temperature (T_m) at 48°C (ΔH = 145 kcal/mol) and a second at 58°C (ΔH = 144 kcal/mol). DSC scans of L260P also show 2 thermal transitions, the first at 48°C (ΔH = 133 kcal/mol) is similar to WT, whereas the second transition shows a 2°C decrease in T_m and a slight reduction in enthalpy (ΔH = 121 kcal/mol). Both proteins precipitated during the course of the experiment, resulting in some uncertainty in the T_m and enthalpy values. The most likely interpretation is that the higher melting domain, which corresponds to the α1-3 repeats,[39] is slightly destabilized, whereas there is not significant perturbation of the lower melting domain, which corresponds to repeats α4-5.[39] Repeated thermal denaturation up to 50°C shows that the α4-5 domains are able to unfold reversibly (supplemental Figure 2) and irreversible protein aggregation only occurs when the second domain denatures. The WT and L260P mutant proteins exhibit high helical (~90%) content for both dimers and tetramers, as indicated by circular dichroism (Figure 2B-C), which measures secondary structure. The similar spectra for WT and mutant proteins indicates that introduction of the L260P mutation into the mini-spectrin construct did not significantly affect the secondary structure, that is, the percentage of α-helix.

High-performance liquid chromatography gel filtration, which separates proteins based on their solution size and shape (hydrodynamic radius), was used to determine the relative amounts of tetramers and dimers and potential shape changes induced by the L260P mutation. The mini-spectrins were evaluated by incubating them at 37°C for varying times in physiological buffer. Purified dimer fractions or tetramer fractions from either WT or L260P were injected onto the high-performance liquid chromatography column, which was maintained at room temperature (~20-23°C), immediately after purification or after incubation at 37°C for 45 (data not shown) or 90 minutes (Figure 2D-E). No differences in elution profile were noted for the 45- and 90-minute time points, indicating equilibrium was achieved within 45 minutes at 37°C. This is in agreement with previously published data for full-length spectrin showing that dimer-tetramer equilibrium is achieved on the order of 45 minutes at 37°C, on the order of hours at 23°C, and on the order of many days at 4°C, further demonstrating the similarity of the mini-spectrin and full-length protein in terms of tetramerization.[40] Critical evaluation of the equilibrated samples (Figure 2D-E, lower panels) shows that the relative ratios of dimer and tetramer are the same regardless of whether the initial purified sample was tetramer or dimer, as expected for a reversible equilibrium. Furthermore, L260P contains a higher percentage of dimer than the WT protein at the same concentration, consistent with the lower K_d observed in the sedimentation equilibrium experiments. Finally, the later elution of both the tetramer and dimer peaks for the L260P protein indicate that the mutant protein is a more compact and/or more flexible structure because later elution is indicative of somewhat smaller hydrodynamic radii.

Chemical crosslinking of L260P and WT dimers and tetramers

L260P dimers and tetramers were chemically crosslinked with EDC/NHS at 0°C and room temperature in parallel with WT controls. This "zero-length" reaction covalently links amines (N terminus α-amino group and ε-amino group of Lys) to carboxyl groups (C terminus carboxyl group, and side chain carboxyl groups of Asp or Glu) that are within salt-bridging distances. Allowing for side chain lengths, this requires that the α-carbons of the crosslinked residues be within approximately 12 Å. After the crosslinking reaction was quenched, the samples were subjected to SDS-PAGE (Figure 3A; supplemental Figure 3). The respective dimer or tetramer bands from each time point were excised from the gel, subjected to tryptic digestion, then analyzed on an LTQ-Orbitrap XL mass spectrometer.

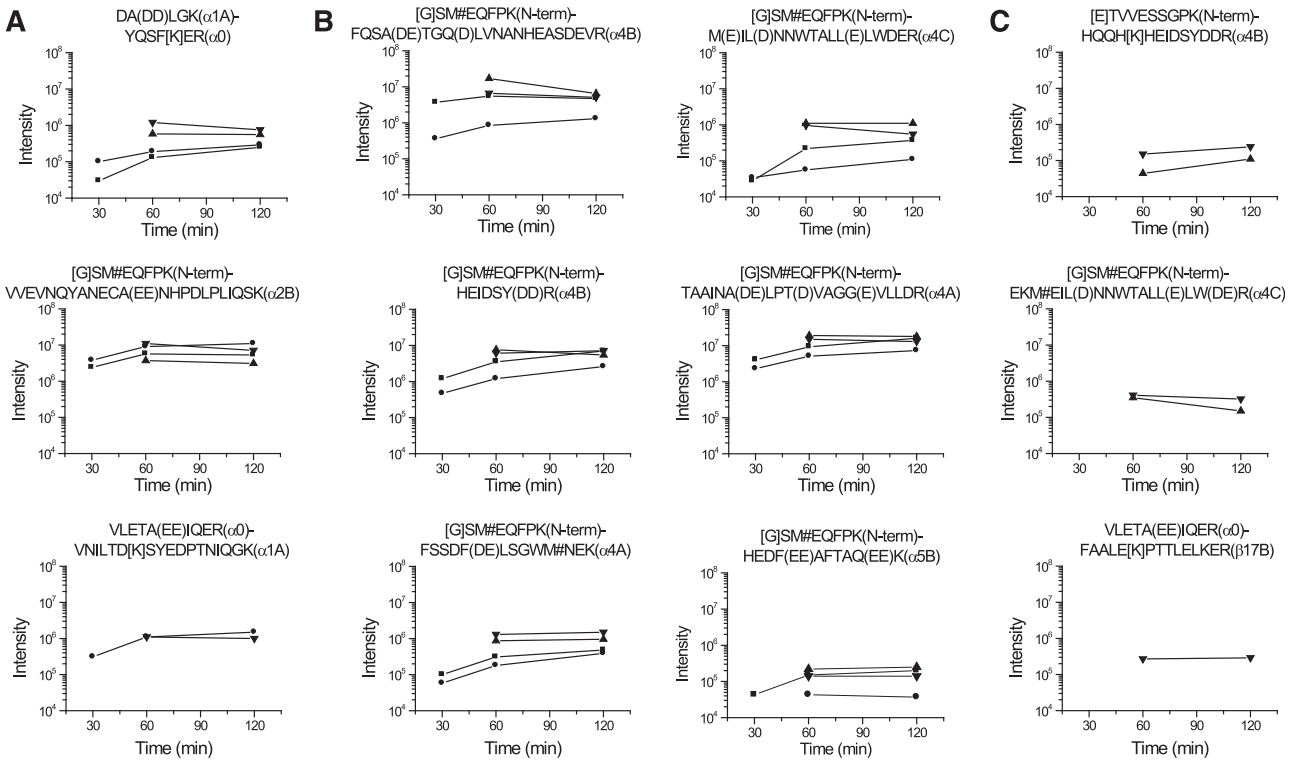

Figure 4. Quantitation of mini-spectrin dimer crosslinks. The intensity (log scale) of each crosslinked peptide is plotted for each time point as follows: ■, WT 0°C; ●, WT RT; ▲L260P, 0°C; ▼, L260P RT. (A) Crosslinked peptides consistent with an open dimer conformation. (B) Crosslinked peptides consistent with a closed dimer conformation. (C) Crosslinked peptides unique to L260P and consistent with a closed dimer conformation.

Characterization of crosslinks in L260P dimers

Chemical crosslinking coupled with MS allows identification of closely associated amino acid side chains. In the case of the crosslinker used here, an acidic and basic group must be within salt bridge distances to react. Comparison of the crosslinks observed and the amount (intensity) of each was used to estimate the relative amounts of open or closed dimer in WT and L260P mini-spectrin dimers and to identify conformational changes. The most informative crosslinks for analyzing the L260P mutant were those indicative of open dimers, indicative of closed dimers, or unique to the L260P mutant. Three crosslinks were identified that were indicative of an open dimer conformation (Figure 3B; supplemental Table 1). Quantitation of these crosslinks (Figure 4A) showed that they were observed with both WT and L260P dimers, and crosslink VLETAEEIQER(α0)-VNILTDKSYEDPTNIQGK(α1A) was only observed at room temperature. Yields of the other 2 crosslinks were higher at room temperature for both WT and L260P, consistent with the prior observation that the closed ↔ open dimer equilibrium shifts toward open dimers at higher temperatures.[40] Nine crosslinks consistent with closed dimers were observed (Figure 3C; supplemental Table 1). Six of these crosslinks were observed for both WT and L260P (Figure 4B), whereas 3 were specific to L260P (Figure 4C). All of the closed dimer-specific crosslinks involved the N terminus of α-spectrin or a peptide from this flexible tail region, which has been previously identified as a highly mobile, relatively disordered region based upon nuclear magnetic resonance (NMR) structures of α-spectrin recombinant fragments.[41] Overall, yields of most crosslinks indicative of closed dimers are higher for the L260P mutant than for WT dimers; this, together with the more compact hydrodynamic radius of the L260P dimer, suggests that this mutant has substantially shifted the open ↔ closed dimer equilibrium toward the closed dimer state. Stabilization of dimers in the closed conformation by the L260P mutation is further supported by mutant dimer-specific crosslinks (Figure 3D), particularly the crosslink between the α1 and α3 domains, which suggests that these 2 domains more tightly laterally associate compared with WT closed dimers. All other L260P dimer-specific variants are in the vicinity of the mutation and are suggestive of substantial conformational changes within α2 and between α2 and α3 (Figure 3D; supplemental Table 2). Several representative spectra of L260P specific crosslinks are shown in supplemental Figures 4-6.

Characterization of crosslinks in L260P tetramers

Chemical crosslinking-MS was also used to identify closely associated residues in WT and L260P tetramers in order to identify changes in protein conformation induced by the mutation. The most interesting L260P mini-spectrin tetramer crosslinks are those unique to the mutant. However, it is also informative that 25 of 35 crosslinks were observed in both WT and L260P tetramers, indicating most regions of the protein did not undergo significant conformational changes. Analogous to results for the mutant dimer, most of the 10 mutant-specific crosslinks involved the α2 domain that harbors the mutation (supplemental Table 3). The 6 most informative crosslinks are shown in Figure 5A and Table 2. Importantly, 3 L260P-specific crosslinks were between residues that were 43-76 Å apart in the WT protein, as illustrated by mapping these mutations onto a structure of the WT tetramer (Figure 5B; representative spectra are shown in supplemental Figures 7 and 8). This WT structure was used as a template for modeling the structural changes indicated by these crosslinks. It was not possible to derive a single stable structure

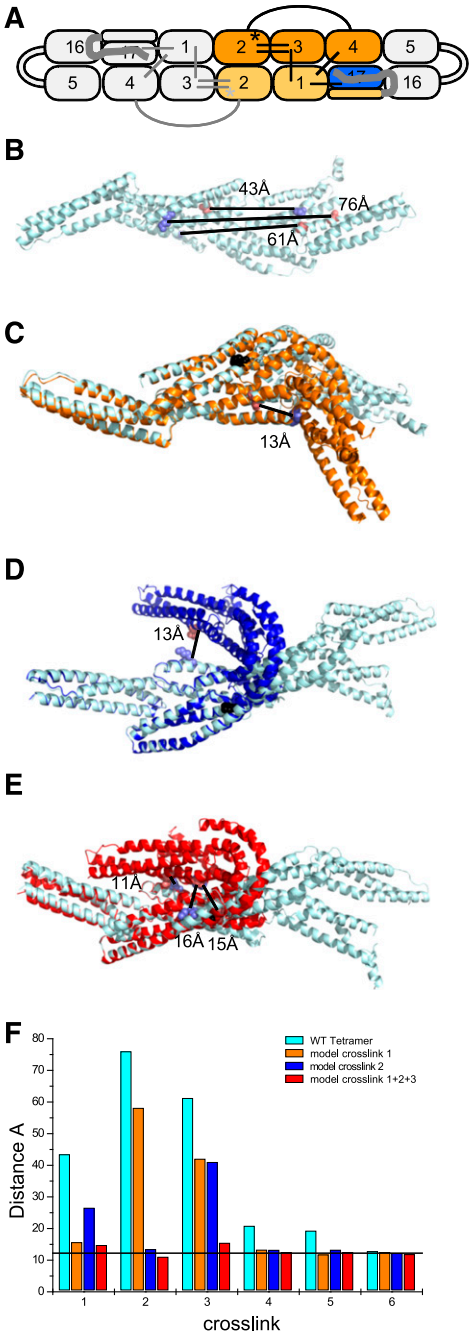

Figure 5. Long-range crosslinks unique to the L260P tetramer. (A) Schematic representation of 6 key crosslinks (black lines in right half of model; these crosslinks are repeated as gray lines in the left half of the model, which is a mirror image of the right half) unique to L260P tetramers (Table 2). The colored region indicates repeats used for modeling structural changes required to accommodate distance constraints imposed by L260P-specific crosslinks. (B) A structural model of the colored region of WT mini-spectrin. Locations of 3 L260P tetramer-specific crosslinks (Table 2; crosslinks 1-3) and the distances between the crosslinked residues in the WT structure are highlighted. Crosslinked side chains are presented using spheres (blue, K; red, D or E). (C-E) The light cyan WT tetramer model (B) is superimposed on alternative L260P structures. (C) The model shown in orange was derived by applying the distance constraint defined by crosslink 1 in panel B (residues 508-364). The black sphere shows the location of the L260P mutation. (D) The model shown in blue was derived by applying the distance constraint defined by crosslink 2 in panel B (residues 265-466). (E) The model shown in red was derived by first applying crosslink 2 followed by crosslinks 1 and 3. (F) The distances between α-carbons for 6 key L260P tetramer-specific crosslinked residues on the models are shown in panels B-E. The horizontal line at 12 Å defines the expected maximum distance between α-carbons of residues capable of being crosslinked by a zero-length crosslinking reagent.

that satisfied the distance constraints for all crosslinks simultaneously. The most feasible ensemble of mutant structures is shown in Figure 5C-E. Distances between the α-carbons of crosslinked residues for the different models are shown in Figure 5F. Taken together, these data indicate that the region in the vicinity of the mutation is unusually flexible and dynamic because it most likely adopts multiple alternative conformations. All of these conformations preserve the high helical content, indicated by the circular dichroism measurements, and all conformations involve a large kink between α2 and α3 that is consistent with the smaller hydrodynamic radius observed in the L260P mutant compared with the WT mini-spectrin (Figure 2D).

Discussion

Most HE and HPP patients have mutations in red cell spectrin that destabilize tetramer formation; the resulting reduced number of spectrin crosslinks bridging between junctional complexes weakens the membrane skeleton. The most intriguing HE/HPP mutations are those located substantial distances from the tetramerization site because the mechanisms by which these distal mutations reduce tetramer formation and destabilize red cell membranes are not known. Because of the very large size of full-length spectrin polypeptide chains, structural and functional analyses of hereditary anemia-associated mutations in the context of full-length recombinant spectrin have been impractical. Thus, we developed a mini-spectrin recombinant protein as a template to study properties of mutant spectrin tetramerization in a more physiological context than the more commonly used head-to-head univalent association of individual α and β recombinant fragments. Importantly, this mini-spectrin undergoes the open-closed dimer equilibrium and the bivalent dimer-tetramer equilibrium with similar apparent tetramer affinity to that of the full-length molecule.[27]

Understanding the specific mechanisms underlying mutations in erythrocyte spectrin and careful development of physiologically pertinent mini-spectrins are critical for both understanding the pathobiology of disease and for designing rationale strategies for therapeutic interventions. Such strategies are being successfully pursued for dystrophin and uterotrophin, which are large, membrane-associated spectrin repeat–containing proteins associated with muscular dystrophy.[42,43] As with erythrocyte spectrin, their large size makes them difficult to synthesize for biologic studies and prohibits their use in most gene therapy vectors.[44] Furthermore, mini-dystrophins have proven to be very promising in recent gene therapy trials.[45,46]

The moderate perturbation in thermal denaturation (Figure 2A) and the lack of significant changes in secondary structure (Figure 2B-C) for the L260P mutation suggest that structural destabilization is relatively minor and localized. These observations are consistent with prior results using mild proteolysis to characterize mutant spectrin from patients with HE and HPP because proteolysis of spectrin from L260P patients showed protease susceptibility only increased in the immediate vicinity of the mutation.[38,47-49] The chemical crosslinking data also are consistent with relatively moderate structural changes that are limited to the vicinity of the mutation because all crosslinks observed in the WT protein were also observed in the L260P mutant. The additional crosslinks unique to the mutant were either indicative of the shift toward closed dimers or in the vicinity of the mutation (Figures 3 and 5).

Table 2. Key crosslinks unique to the L260P tetramer

Number	Residue	Crosslinked peptides*	Spectrin domain	MH+	Error (ppm)	z
1	508-364	AHI(EE)LR-HEAFE[K]STASWAER	α1C-β17B	2497.222	3.04	4
2	265-466	HEIDSY(DD)*R*-YQ[K]HQSLEAEVQTK	α4B-α1B	2819.323	1.70	4
3	276-39	FQSADETGQ[D]LVNANHEASDEVR-TEVLH[K]K	α4B-α2B	3367.615	3.80	4
4	35-170	T[E]VLHK-AE[K]LTLSHPSDAPQIQEM#K	α2B-α3B	2846.472	1.97	4
5	35-167	T[E]VLHK-ELCA[K]AEK	α2B-α3B	1655.878	0.00	3
6	437-170	DA(DD)LGK-AE[K]LTLSHPSDAPQIQEM#K	α1A-α3B	2853.393	1.12	4

MH+, protonated molecular ion mass.
*[X], crosslinked residue; (X), ambiguous assignment crosslinked residue; #, methionine oxidation.

The crosslinking data yielded additional important insights into changes in the tertiary conformation of the mutant dimers and tetramers. Several mutation-specific crosslinks are of particular interest. One crosslink between α1 and α3 indicates these 2 domains are in closer proximity in the mutant dimer compared with WT, consistent with the smaller hydrodynamic radius observed in gel filtration experiments (Figure 2D). Also, structural modeling was used to further explore the crosslinks observed in the L260P tetramer that were long distances apart in the WT structure. These mutant-specific crosslinks indicate substantial changes in the tertiary structure in order to bring these residues into close enough proximity for crosslinking to occur (Figure 5). Also, the inability to converge on a single model that satisfied all distance constraints simultaneously suggests that the actual structure of the mutant protein is most likely an ensemble of multiple conformations as shown in Figure 5C-E.

The differences observed for the L260P and Q471P mutations suggest that the mechanisms of tetramer destabilization are more dependent upon the location within the spectrin molecule than on analogous locations within different spectrin repeats. The differing mechanisms for the L260P and Q471P mutants fit schematic models of closed and open dimers (Figure 1B). As illustrated, the closed-open dimer conformational rearrangement is likely to involve flexing of hinges or other conformational rearrangements between α1 and α2 as well as α2 and α3. Hence, it is not surprising that the L260P mutation, which is located next to the α2-α3 connector, affects the closed-open dimer equilibrium as demonstrated in this study. In contrast, the Q471P mutation, which is located next to the α4-α5 connector, does not significantly affect this equilibrium because it is quite distal from the domains involved in the closed-open dimer conformational changes. Taken together, these results predict that other HE and HPP mutations located in the α-spectrin domains 1-3 might destabilize tetramer formation by favoring closed dimers, whereas mutations outside this region are likely to destabilize red cell membranes by alternative mechanisms.

Acknowledgments

The authors thank P. Hembach for technical assistance, M. Fuller for editorial assistance, the Wistar Institute Proteomics Core for mass spectrometry analyses, and the Children's Hospital of Philadelphia Protein Core Facility for use of their circular dichroism instrument.

This work was supported by the National Institutes of Health Heart, Lung and Blood Institute grants (HL038794) (D.W.S.) and (HL065449) (P.G.G.); a National Cancer Institute core grant (CA010815) (Wistar Institute); and a Philadelphia Health Care Trust Fellowship (S.S.).

Authorship

Contribution: S.L.H. and S.S. designed and performed research, analyzed and interpreted data, and drafted the manuscript; H.-Y.T. performed research and assisted with data analysis/interpretation; M.G. performed research and data interpretation; P.G.G. prepared the wild-type and mutant expression plasmids, assisted with data interpretation, and reviewed/edited the manuscript; and D.W.S. designed and directed the research and assisted with data interpretation, manuscript preparation, and manuscript editing.

Conflict-of-interest disclosure: The authors declare no competing financial interests.

Correspondence: David W. Speicher, The Wistar Institute, 3601 Spruce St, Philadelphia, PA 19104; e-mail: speicher@wistar.org.

References

1. Delaunay J. The molecular basis of hereditary red cell membrane disorders. *Blood Rev.* 2007;21(1):1-20.
2. Gallagher PG, Forget BG. Hematologically important mutations: spectrin variants in hereditary elliptocytosis and hereditary pyropoikilocytosis. *Blood Cells Mol Dis.* 1996;22(3):254-258.
3. Bennett V, Gilligan DM. The spectrin-based membrane skeleton and micron-scale organization of the plasma membrane. *Annu Rev Cell Biol.* 1993;9:27-66.
4. Bennett V, Baines AJ. Spectrin and ankyrin-based pathways: metazoan inventions for integrating cells into tissues. *Physiol Rev.* 2001;81(3):1353-1392.
5. Morrow JS, Marchesi VT. Self-assembly of spectrin oligomers in vitro: a basis for a dynamic cytoskeleton. *J Cell Biol.* 1981;88(2):463-468.
6. Delaunay J, Dhermy D. Mutations involving the spectrin heterodimer contact site: clinical expression and alterations in specific function. *Semin Hematol.* 1993;30(1):21-33.
7. Gallagher PG. Hereditary elliptocytosis: spectrin and protein 4.1R. *Semin Hematol.* 2004;41(2):142-164.
8. Discher DE, Winardi R, Schischmanoff PO, Parra M, Conboy JG, Mohandas N. Mechanochemistry of protein 4.1's spectrin-actin-binding domain: ternary complex interactions, membrane binding, network integration, structural strengthening. *J Cell Biol.* 1995;130(4):897-907.
9. Baines AJ. The spectrin-ankyrin-4.1-adducin membrane skeleton: adapting eukaryotic cells to the demands of animal life. *Protoplasma.* 2010;244(1-4):99-131.
10. Dick KA, Ikeda Y, Day JW, Ranum LP. Spinocerebellar ataxia type 5. *Handb Clin Neurol.* 2012;103:451-459.
11. Goellner B, Aberle H. The synaptic cytoskeleton in development and disease. *Dev Neurobiol.* 2012;72(1):111-125.
12. Ipsaro JJ, Huang L, Mondragón A. Structures of the spectrin-ankyrin interaction binding domains. *Blood.* 2009;113(22):5385-5393.
13. Ipsaro JJ, Mondragón A. Structural basis for spectrin recognition by ankyrin. *Blood.* 2010;115(20):4093-4101.
14. Stabach PR, Simonović I, Ranieri MA, et al. The structure of the ankyrin-binding site of beta-spectrin reveals how tandem spectrin-repeats generate unique ligand-binding properties. *Blood.* 2009;113(22):5377-5384.

15. Grum VL, Li D, MacDonald RI, Mondragón A. Structures of two repeats of spectrin suggest models of flexibility. *Cell.* 1999;98(4):523-535.

16. Choi HJ, Weis WI. Crystal structure of a rigid four-spectrin-repeat fragment of the human desmoplakin plakin domain. *J Mol Biol.* 2011; 409(5):800-812.

17. Kusunoki H, MacDonald RI, Mondragón A. Structural insights into the stability and flexibility of unusual erythroid spectrin repeats. *Structure.* 2004;12(4):645-656.

18. Kusunoki H, Minasov G, Macdonald RI, Mondragón A. Independent movement, dimerization and stability of tandem repeats of chicken brain alpha-spectrin. *J Mol Biol.* 2004; 344(2):495-511.

19. Ylänne J, Scheffzek K, Young P, Saraste M. Crystal structure of the alpha-actinin rod reveals an extensive torsional twist. *Structure.* 2001;9(7): 597-604.

20. Zhang Z, Weed SA, Gallagher PG, Morrow JS. Dynamic molecular modeling of pathogenic mutations in the spectrin self-association domain. *Blood.* 2001;98(6):1645-1653.

21. Gaetani M, Mootien S, Harper S, Gallagher PG, Speicher DW. Structural and functional effects of hereditary hemolytic anemia-associated point mutations in the alpha spectrin tetramer site. *Blood.* 2008;111(12):5712-5720.

22. Knowles WJ, Bologna ML, Chasis JA, Marchesi SL, Marchesi VT. Common structural polymorphisms in human erythrocyte spectrin. *J Clin Invest.* 1984;73(4):973-979.

23. Gallagher PG, Tse WT, Coetzer T, et al. A common type of the spectrin alpha I 46-50a-kD peptide abnormality in hereditary elliptocytosis and pyropoikilocytosis is associated with a mutation distant from the proteolytic cleavage site. Evidence for the functional importance of the triple helical model of spectrin. *J Clin Invest.* 1992; 89(3):892-898.

24. Gallagher PG, Forget BG. Spectrin St Louis and the alpha LELY allele. *Blood.* 1994;84(5):1686-1687.

25. Johnson CP, Gaetani M, Ortiz V, et al. Pathogenic proline mutation in the linker between spectrin repeats: disease caused by spectrin unfolding. *Blood.* 2007;109(8):3538-3543.

26. Glele-Kakai C, Garbarz M, Lecomte MC, et al. Epidemiological studies of spectrin mutations related to hereditary elliptocytosis and spectrin polymorphisms in Benin. *Br J Haematol.* 1996; 95(1):57-66.

27. Harper SL, Li D, Maksimova Y, Gallagher PG, Speicher DW. A fused alpha-beta "mini-spectrin" mimics the intact erythrocyte spectrin head-to-head tetramer. *J Biol Chem.* 2010;285(14): 11003-11012.

28. Beer LA, Tang HY, Sriswasdi S, Barnhart KT, Speicher DW. Systematic discovery of ectopic pregnancy serum biomarkers using 3-D protein profiling coupled with label-free quantitation. *J Proteome Res.* 2011;10(3):1126-1138.

29. Neubert H, Bonnert TP, Rumpel K, Hunt BT, Henle ES, James IT. Label-free detection of differential protein expression by LC/MALDI mass spectrometry. *J Proteome Res.* 2008;7(6): 2270-2279.

30. Sali A, Blundell TL. Comparative protein modelling by satisfaction of spatial restraints. *J Mol Biol.* 1993;234(3):779-815.

31. Fiser A, Do RK, Sali A. Modeling of loops in protein structures. *Protein Sci.* 2000;9(9): 1753-1773.

32. Martí-Renom MA, Stuart AC, Fiser A, Sánchez R, Melo F, Sali A. Comparative protein structure modeling of genes and genomes. *Annu Rev Biophys Biomol Struct.* 2000;29:291-325.

33. Eswar N, Webb B, Marti-Renom MA, et al. Comparative protein structure modeling using Modeller. *Curr Protoc Bioinformatics.* 2006; Chapter 5:Unit 5.6.

34. Li D, Harper SL, Tang HY, Maksimova Y, Gallagher PG, Speicher DW. A comprehensive model of the spectrin divalent tetramer binding region deduced using homology modeling and chemical cross-linking of a mini-spectrin. *J Biol Chem.* 2010;285(38):29535-29545.

35. Shahbakhti F, Gratzer WB. Analysis of the self-association of human red cell spectrin. *Biochemistry.* 1986;25(20):5969-5975.

36. Ungewickell E, Gratzer W. Self-association of human spectrin. A thermodynamic and kinetic study. *Eur J Biochem.* 1978;88(2):379-385.

37. Ralston GB. Temperature and pH dependence of the self-association of human spectrin. *Biochemistry.* 1991;30(17):4179-4186.

38. Marchesi SL, Letsinger JT, Speicher DW, et al. Mutant forms of spectrin alpha-subunits in hereditary elliptocytosis. *J Clin Invest.* 1987;80(1): 191-198.

39. An X, Guo X, Zhang X, et al. Conformational stabilities of the structural repeats of erythroid spectrin and their functional implications. *J Biol Chem.* 2006;281(15):10527-10532.

40. DeSilva TM, Peng KC, Speicher KD, Speicher DW. Analysis of human red cell spectrin tetramer (head-to-head) assembly using complementary univalent peptides. *Biochemistry.* 1992;31(44): 10872-10878.

41. Park S, Caffrey MS, Johnson ME, Fung LW. Solution structural studies on human erythrocyte alpha-spectrin tetramerization site. *J Biol Chem.* 2003;278(24):21837-21844.

42. Lin AY, Prochniewicz E, Henderson DM, Li B, Ervasti JM, Thomas DD. Impacts of dystrophin and utrophin domains on actin structural dynamics: implications for therapeutic design. *J Mol Biol.* 2012;420(1-2):87-98.

43. Teichmann MD, Wegner FV, Fink RH, et al. Inhibitory control over Ca(2+) sparks via mechanosensitive channels is disrupted in dystrophin deficient muscle but restored by mini-dystrophin expression. *PLoS ONE.* 2008; 3(11):e3644.

44. Tang Y, Cummins J, Huard J, Wang B. AAV-directed muscular dystrophy gene therapy. *Expert Opin Biol Ther.* 2010;10(3):395-408.

45. Verhaart IE, Aartsma-Rus A. Gene therapy for Duchenne muscular dystrophy. *Curr Opin Neurol.* 2012;25(5):588-596.

46. Bowles DE, McPhee SW, Li C, et al. Phase 1 gene therapy for Duchenne muscular dystrophy using a translational optimized AAV vector. *Mol Ther.* 2012;20(2):443-455.

47. Sahr KE, Tobe T, Scarpa A, et al. Sequence and exon-intron organization of the DNA encoding the alpha I domain of human spectrin. Application to the study of mutations causing hereditary elliptocytosis. *J Clin Invest.* 1989;84(4): 1243-1252.

48. Speicher DW, Marchesi VT. Spectrin domains: proteolytic susceptibility as a probe of protein structure. *J Cell Biochem.* 1982;18(4):479-492.

49. Speicher DW, Morrow JS, Knowles WJ, Marchesi VT. Identification of proteolytically resistant domains of human erythrocyte spectrin. *Proc Natl Acad Sci USA.* 1980;77(10):5673-5677.

50. Ursitti JA, Kotula L, DeSilva TM, Curtis PJ, Speicher DW. Mapping the human erythrocyte beta-spectrin dimer initiation site using recombinant peptides and correlation of its phasing with the alpha-actinin dimer site. *J Biol Chem.* 1996;271(12):6636-6644.